ISSN: 1001-4055 Vol. 46 No. 04 (2025)

Influence of MSW landfill site on Seismic Response of RC Buildings considering Soil Structure Interaction under far field and near field Earthquake

Mr. Pruthviraj S R 1*, Dr. K. Manjunatha 2 and Dr. C M Ravi Kumar 3

¹ Research Scholar, DoS in Civil Engineering, University BDT College of Engineering, Davanagere, Karnataka, India-577004

² Professor, DoS in Civil Engineering, University BDT College of Engineering, Davanagere, Karnataka, India-577004

³ Associate

Professor, DoS in Civil Engineering, University BDT College of Engineering, Davanagere, Karnataka, India-577004

*Corresponding Author: Mr. Pruthviraj S R , DoS in Civil Engineering, University BDT College of Engineering, Davanagere, Karnataka, India-577004

Email: pruthvi960637@gmail.com, ORCID: https://orcid.org/0000-0001-9919-0411

Abstract

The kind of challenging soil conditions adopted for this analysis is Landfill Site (LFS) condition to evaluate the seismic response of RC buildings considering soil structure interaction. The results of the pile cap, storey lateral displacement, and inter-story drift, story accelaration need to be obtained for soil-structure interaction on Landfill Site supported structure and compared with the rigid base structural response. The impact of LFS on the seismic response of multistorey buildings is a critical consideration in modern Civil Engineering. This study focuses on investigating the seismic behavior of multistorey buildings constructed on Landfill Site (LFS), with a particular emphasis on soil-structure interaction (SSI). Advanced tools such as ETABS, CSI Detailing, and ABAQUS CAE are employed for the design, detailing, and SSI analysis, respectively. The low rise (G+4), mid-rise (G+14) and high rise (G+24) storey building situated on Landfill Site (LFS) deposites is adopted for this research. The analysis includes a detailed comparison between buildings constructed on natural soil versus those on challenging soil site like landfill sites, examining the influence of varying soil properties on the seismic response. A key aspect of the research is the validation of results using experimental data and comparisons with findings from previous studies, ensuring the reliability of the conclusions drawn.

Keywords: Soil-Structure Interaction, Non-linear time history analysis Etabs, Abaqus, Landfill Site (LFS), dynamic properties of soil.

Introduction

The soil-structure interaction (SSI) is the process of understanding the exchange of forces between the soil and structure under external loads such as machine vibration, blast, wind, or seismic events. Under seismic effects, both the soil and structure experience ground motion, transferring acceleration that induces vibration and potential structural damage or collapse. SSI is crucial in seismic-prone areas, as soil response influences structural failure modes like shear, flexure, torsion. Designing structures on challenging soils such as MSW landfill sites is

complex, requiring seismic analysis using site-specific earthquake data (PGA) to enhance warning time before failure.

Multi-storey buildings in earthquake zones use different foundation types—shallow or pile—based on soil conditions and load requirements. Traditional seismic analysis assumes fixed-base support, suitable for rock foundations but inaccurate for soft soils where dynamic soil deformation occurs. SSI considers mutual influences between soil and structure (Kramer, 1996; Bowles, 1996). In MSW landfills, seismic loading may cause deformation, liner tearing, or system failures, influenced by waste compaction, moisture, and decomposition. Liquefaction and lateral spreading are potential risks in saturated zones.

To improve SSI understanding at the Mavallipura MSW landfill, Bengaluru, comparisons with major earthquake case studies (Niigata, Mexico City) are insightful. These studies highlight how soft, heterogeneous soils amplify seismic motion. Mavallipura's seismic performance is moderate due to soil improvement measures like vertical drains (Bo et al., 2019).

Objectives of the Study:

- Analyze low-, mid-, and high-rise RC SMRF buildings under fixed-base and SSI conditions using nonlinear time history analysis.
- Incorporate dynamic soil data from the MSW site to assess seismic response.
- Validate analytical models with previous research.
- Investigate foundation type effects on shear, lateral deformation, and performance levels under SSI.

Project site Details

The Mavallipura landfill, located 30 km from Bengaluru, spans about 40.48 hectares and has been overloaded since its operation in 2007, receiving up to 1,000 tonnes of waste daily. The site, composed mostly of uncompacted waste about 6 meters high, poses seismic risks such as liquefaction, lateral spreading, and leachate migration due to poor compaction and high moisture. Dynamic soil properties like shear wave velocity, cohesion, and elasticity may degrade during earthquakes, leading to instability and contamination. The landfill consists of multilayer protection systems with HDPE liners, clay bases, and leachate management networks, but inadequate maintenance increases vulnerability.

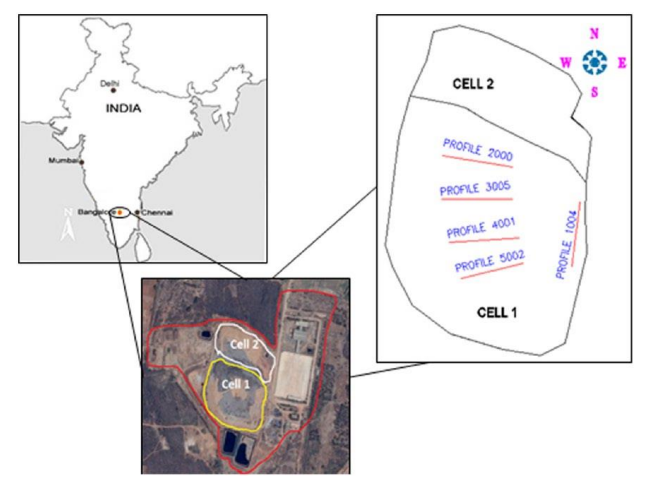


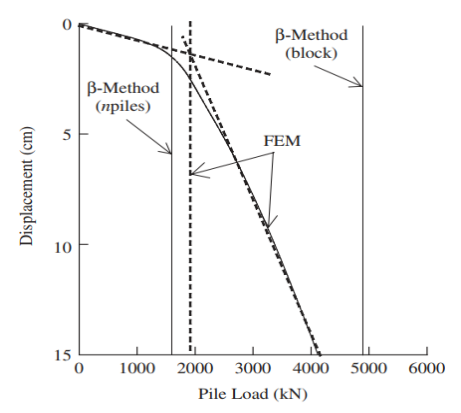
Figure 1. Google map image showing a Mavallipura landfill site with cell 1 and cell 2, and also showing the multichannel analysis of surface waves (MASW) test locations.

To accomplish this objective, a numerical simulation of a soil-structure system was executed using Abaqus 6.12 software, employing a fully coupled nonlinear time history analysis approach. The numerical modeling method utilized in Abaqus (Dassault Systems SIMULIA 2012), offering valuable insights for professionals in both academic and industrial settings. This is particularly relevant given the increasing interest in the application of 3D finite-element modeling for addressing soil-structure interaction challenges in engineering

projects. Numerous researchers(Matinmanesh and Asheghabadi, 2011; Visuvasam and Chandrasekaran, 2019; Shekhar, Tripathi and Ram, 2022) have examined the seismic behavior of soil-pile structure systems by utilizing the direct method for modeling soil-structure interaction, thereby achieving accurate and realistic results. Consequently, due to its effectiveness in capturing the complexities of soil-pile-structure interaction during dynamic analysis, the direct method is employed in this study.

Validation of Modeling

A soil–structure interaction (SSI) analysis was performed in ABAQUS 2024 following Example 8.6 from Sam Helwani's "Applied Soil Mechanics with ABAQUS Applications." A group of four concrete piles (0.6 × 0.6 m, 9.15 m length) embedded in clay soil (c = 0, ϕ = 30°) was modeled using the β -method to determine load capacity. The close match between the simulated and reference load–displacement results confirms the validity of the modeling procedure.



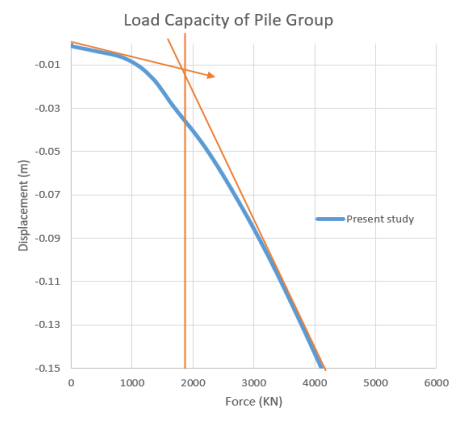


Figure 3: Pile Capacity by Sam Helwani

Figure 4: Pile Capacity by Present Study

Materials Property Details

All structural sections were made from concrete with M-30 grade with a compressive strength (fck) of 35 Mpa. The youngs modulus of the concrete Ec=5000(fck)^{0.5} was 27.386 x10³ Mpa (IS 456, 2000), it had a unit weight of 25 kN/m³ (IS 875 Part-1, 1987) and a steel rebar with Fe-500 grade steel, with a yield strength (fy) of 500 MPa, Modulus of Elasticity for Steel (Es) was 2x10⁵ Mpa (IS 456, 2000) and the density of the rebar was 78.5 kN/m³ (IS 875 Part-1, 1987).

MSW landfill site soil properties.

The below table-1 represents a soil parameters which are adopted for modeling soil in Abaqus, they are adopted from different research journals carried out on the Changi East reclamation.

Table 1: Municipal landfill site soil parameters adopted for analysis

	1 4010 1: 1010	merpar ianam	i site son para	meters adopted to	i anary 515		
Material Properties	Dumped waste		Soil Condit	ion	Reference Journals		
Model	MSW waste	Sandy Soil	Silty clay	Filled up soil			
Depth (mCD) in m	12m	2.0	5.0	3.0	(Arulrajah et al., 2009)		
Sat. Density(kN/m ³)	14	16.5	14.5	18 - 20	(W.Bo et al., 2009)		
Dry Density kN/m³	7.0	15.89	10-14	16.15 -18.1	Pérez, S., & Nunes, L. A. (2017).		
$\rho (kg/m^3)$	1,325.63	1500	800-1200	1,600 to 2,000	$\rho = \frac{Unit\ weight(\ kN/m^3)}{g\ (9.81\ m/s^2)}$		
Specific gravity (Gs)	1.15	2.65	1.15	2.65 - 2.75	(Naveen B. P., Sitharam T. G., et al., 2014).		
Water content % (ω)	30.59	15.30	36	14 - 30%	(Naveen B. P. , Sitharam T. G., et al., 2014)		
Young's Modulus, E (kN/m²)	2230	15,000 - 40,000	10,000- 20,000	30,000 - 50,000	(Naveen B. P., Sitharam T. G., et al., 2014),		
Poisson's ratio	0.3	0.3	0.3	0.3	Smith et al., 2020		
Friction Angle (°) Dilatency Angle (°)	34 5°	32 5°	34 5°	31 5°	(Naveen B. P, 2018)		

ISSN: 1001-4055

Vol. 46 No. 04 (2025)

k (m/day)	3.456×10-7	0.864 m/day	0.0000864 m/	0.01 - 0.1	(W.Bo et al., 2009)
c (kN/m²) Initial void ratio (e ₀)	10 2.5 to 3.0	5 0.5 and 1.5	day 20 2.3	$15 \\ 0.6 - 0.8$	(W.Bo et al., 2009) (Wang et al., 2021)
Void ratio (e)	1.0	0.64	0.4-0.7	0.5-0.7	$e = Gs * \omega$ (Naveen B. P. et al., 2014)
Dynamic shear modulus(G) in MPa	0.8 to 4.2	2 MPa to 4.2 MPa	2 MPa to 4.2 MPa	0.8 – 4.2 MPa	(Naveen B. P., Sitharam T. G., et al., 2014)
Damping ratio	14% to 32%	14% to 18%	10% to 20%	14 - 32%	(Naveen B. P. , Sitharam T. G., et al., 2014)

Loads and Load Combinations considered:

The analysis includes dead, live, and seismic loads with appropriate load combinations. Dead loads from floor finishes, walls, and structural self-weight are automatically computed in ETABS. Live loads are applied as per IS 875 (Part 2) 2.5 kN/m² for floors, 1.5 kN/m² for accessible terraces, and 1 kN/m² for floor finishes. Seismic loads are evaluated using the Modal Nonlinear Time History Method as per IS 1893:2016 in both X and Y directions, with a zone factor of 0.16. The structure, modeled on medium stiff soil, is designed as an SMRF with a response reduction factor of 5. The El Centro time history record is used with a 5% damping ratio to simulate energy dissipation.

Time history data adopted for study

The El Centro (1940) earthquake had a PGA of 0.281g, Mw 6.9, and was a far-field event with moderate shaking. The Northridge (1994) earthquake, despite a slightly lower Mw 6.7, had a much higher PGA of 0.843g due to its near-field nature and closer proximity. These events highlight how hypocentral distance significantly affects ground motion intensity which is represented in table-2.

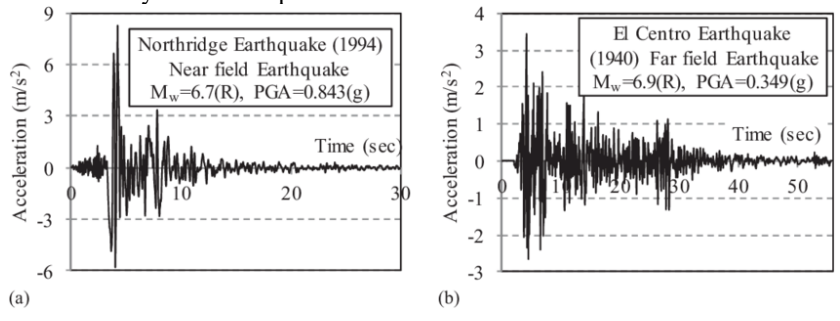


Figure-6: Defining TH Function (a) Northridge Earthquake and (b) El Centro Earthquake Table 2: Adopted Earthquake Records

				-				
Earthquake	Country	Year	PGA (g)	Mw (R)	Duration (s)	Type	Hypo. distance	
Elcentro	US	1940	0.281	6.9	53.72	Far-field	12.2 km	
Northridge	US	1994	0.843	6.7	30	Near Field	9.2 km	

Structural Model and its Details

Structural modeling and its details of low rise, mid rise and high rise buildings were shown in table-3 including thickness of main wall and partition wall details.

Table 3: Building Model details

	8		
Number of the stories	05 (G+4) in (m)	15 (G+14) in (m)	25 (G+24) in (m)
Building	Office	Office	Office
Building type	Low Rise	Medium Rise	High Rise
Each Story Height	3	3	3
Height of the building in m	15	45	75
X and Y direction Bay Width (Column Spacin	4.00	4.00	4.00
C/C)	4.00	4.00	4.00

ISSN: 1001-4055

Vol. 46 No. 04 (2025)

No of Bays in X and Y Dir.	3 no's	3 no's	3 no's
Size of Beam in m	0.23 x 0.45	0.23 x 0.45	0.23 x 0.45
Size of Column (Upto-5 th floor)	0.5×0.5	0.5 x 0.5	0.50×0.50
Size of Column (6 th –10 th floor)		0.45 x 0.45	0.45 x 0.45
Size of Column (11th –15th floor)	-	0.40 x 0.40	0.40 x 0.40
Size of Column (16 th –25 th floor)			0.35×0.35
Thickness of Slab in m	0.150	0.150	0.150
Thickness of the Main, Partition, and Parapet	0.230, 0.150, &	0.230, 0.150, &	0.230, 0.150, &
Wall in m	0.150	0.150	0.150

Boundary conditions for SSI Analysis

The base of the soil is fixed in all 6 degrees of freedom and applied earthquake load onto the base of the soil in X-direction as acceleration in dynamic implicit earthquake step, and the face of the soil is restricted in their relative directions as shown in figure-9.

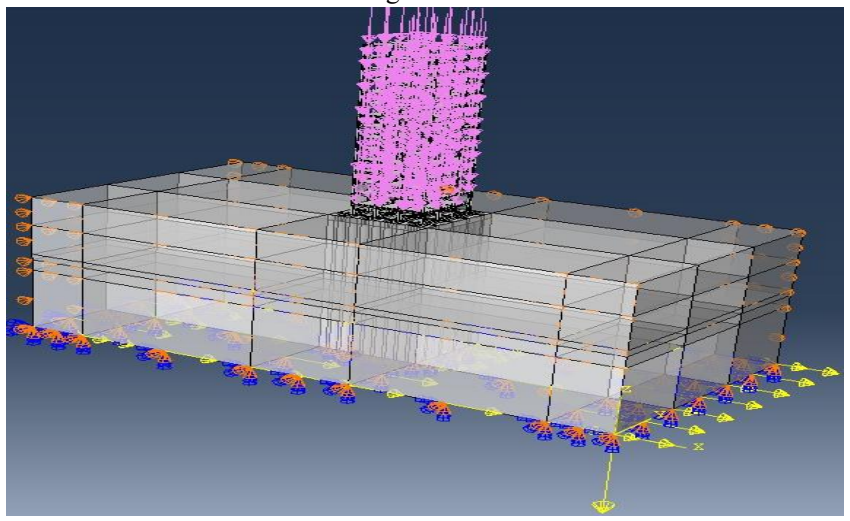


Figure-9: Applied loads for Analysis

A new model was created in ABAQUS CAE by defining geometry for 3D deformable solid parts representing the structure, soil mass, and reinforcement elements. Material properties such as density, Young's modulus, Poisson's ratio, cohesion, and friction angle were assigned to concrete, steel, and soil. The Assembly, Step, and Interaction modules were used to position components, define geostatic, static, and dynamic analysis steps, and apply tie and contact constraints. Boundary conditions fixed the soil base, while earthquake loads were applied through dynamic implicit steps. Structured meshing used C3D8R, B31, and CIN3D8 elements, and the simulation was executed through the Job module.

Analysis and Design Results

The results are presented and discussed in the following sections in terms of Base shear, maximum storey displacement and maximum storey drift for Limit state collapse (LSC) condition and Scaled Time History (STH) for low rise, mid rise and high rise buildings using ETABS software for getting the base reaction from the structural analysis and to get the design design data. Seismic Analysis of Building using ABAQUS for fixed base and Reclamated multilayer soil with and Without Pile and results are plotted in terms of Story Acceleration, Maximum Story Displacement and Maximum Story Displacement.

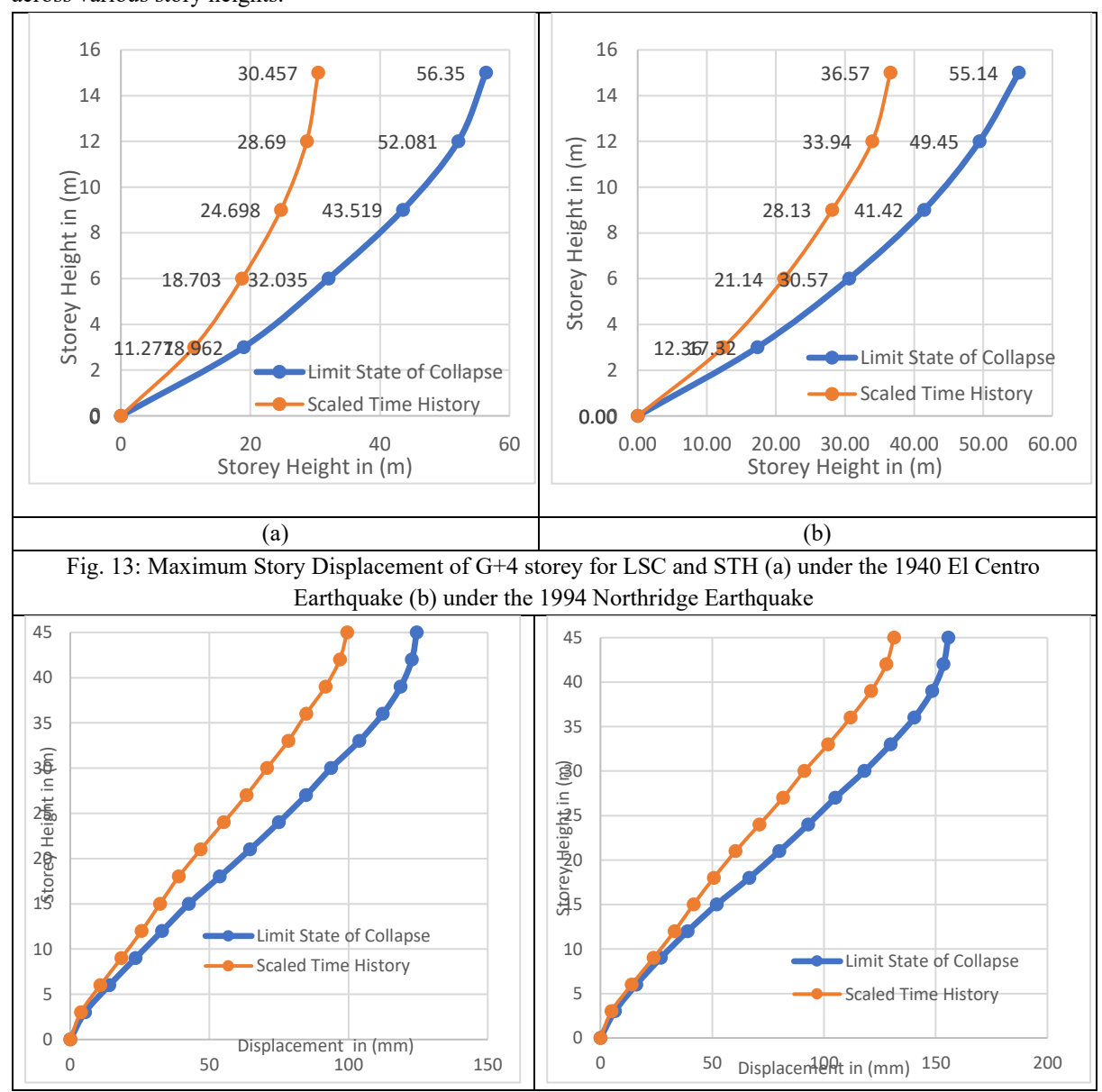
Structural Analysis of low rise, mid rise and high rise buildings and design were performed using ETABS software which was confined to IS456:2000 for concrete frame design and dynamic analysis was done as per IS:1893:2016 considering El-Centro earthquake data collected from PEER Earthquake database. Design results are presented in table-4.

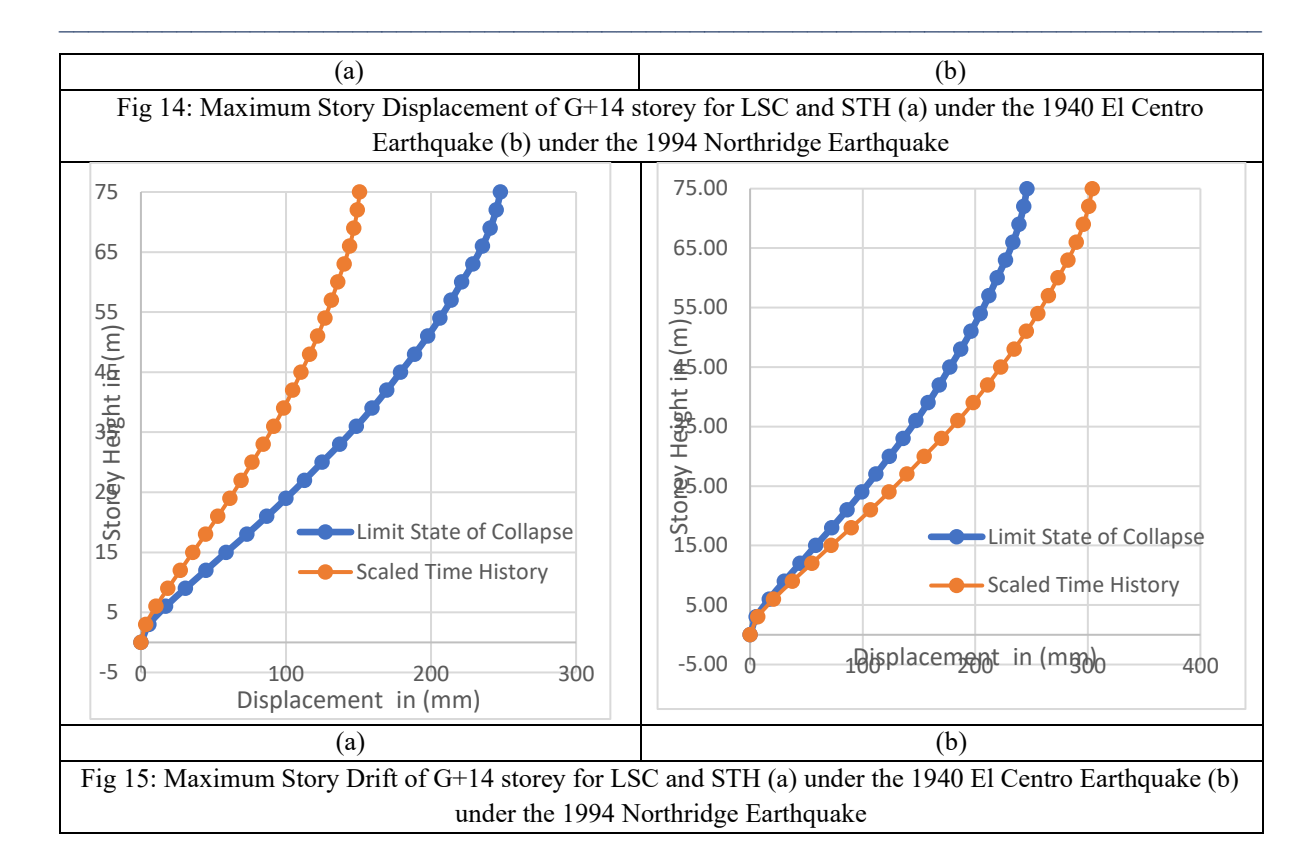
Section Pile Column details on respective floors Beam			Pile
---	--	--	------

Type	Pile Raft Footing		1 to 5	6 to 10	11 to 15	16 to 25	For all s	story
Dimensi on (m)	1m Depth	0.5 Diameter	0.5x 0.5	0.45 x 0.45	0.40 x 0.40	0.35 x 0.35	0.23 x 0.45	0.15m Thick
Rebar N#bar	25@400 (Top) 25@300 (Bot.)	8 #20	12#25	12#20	12#20	12#20	3#16 (Top) 3#16 (Bot.)	10@150
Tie rebars bar@spac.		10@150	10@150	10@150	10@150	10@150	10@150	

Maximum Story Displacement

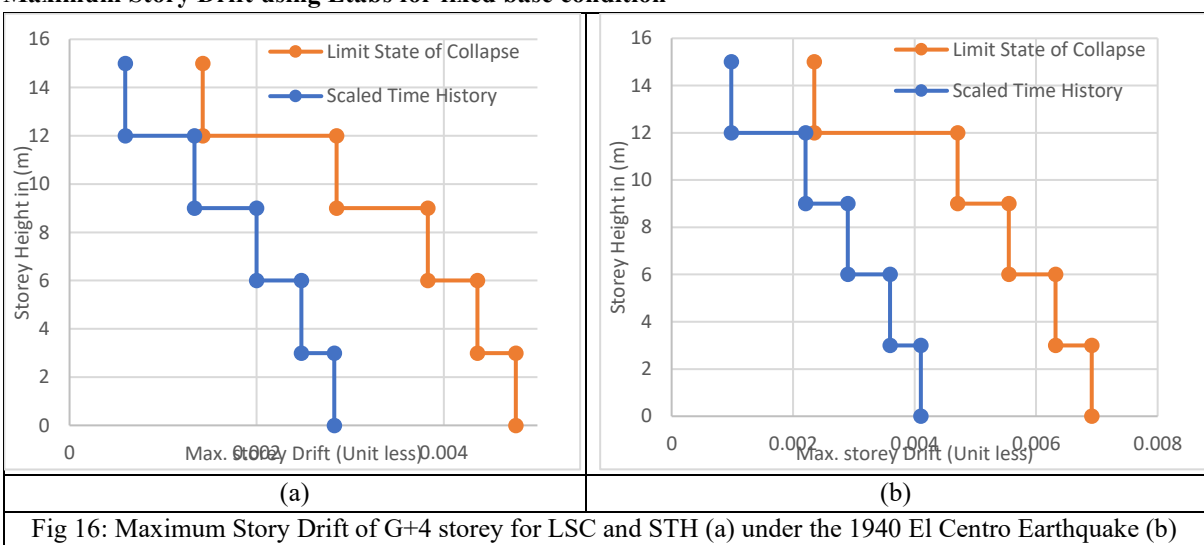
The following graph of G+4 storey, G+14 storey & G+24 storey buildings compares the maximum story displacement of a multistory building under two different seismic loading conditions: the Limit State of Collapse (LSC) and Scaled Time History (STH). The results illustrate how these two conditions affect the displacement across various story heights.





In the Limit State of Collapse (LSC) condition, maximum displacements of 56.35 mm, 124.49 mm, and 247.87 mm were observed at the top stories of G+4, G+14, and G+24 buildings, respectively, all within permissible limits. Under the Scaled Time History (STH) condition, displacements were slightly lower at 30.46 mm, 99.48 mm, and 150.83 mm, reflecting realistic seismic behavior. As per IS 1893 (Part 1): 2016, the allowable limits are 60 mm, 180 mm, and 300 mm for G+4, G+14, and G+24 structures. Both LSC and STH results confirm compliance with code requirements and ensure structural safety.

Maximum Story Drift using Etabs for fixed base condition



The graph compares maximum story drift for Elcentro and Northridge earthquakes under LSC and STH scenarios. For Elcentro, peak drift occurs at the 2nd floor with 0.004769 (LSC) and 0.002829 (STH), while Northridge shows higher peaks of 0.006915 (LSC) and 0.00410 (STH). This represents an increase of about 45%, indicating greater lateral deformation under Northridge, especially in lower-mid stories. The results emphasize

under the 1994 Northridge Earthquake

the need for enhanced drift control and reinforcement at critical story levels to ensure stability during strong seismic events.

For G+14 storey Building

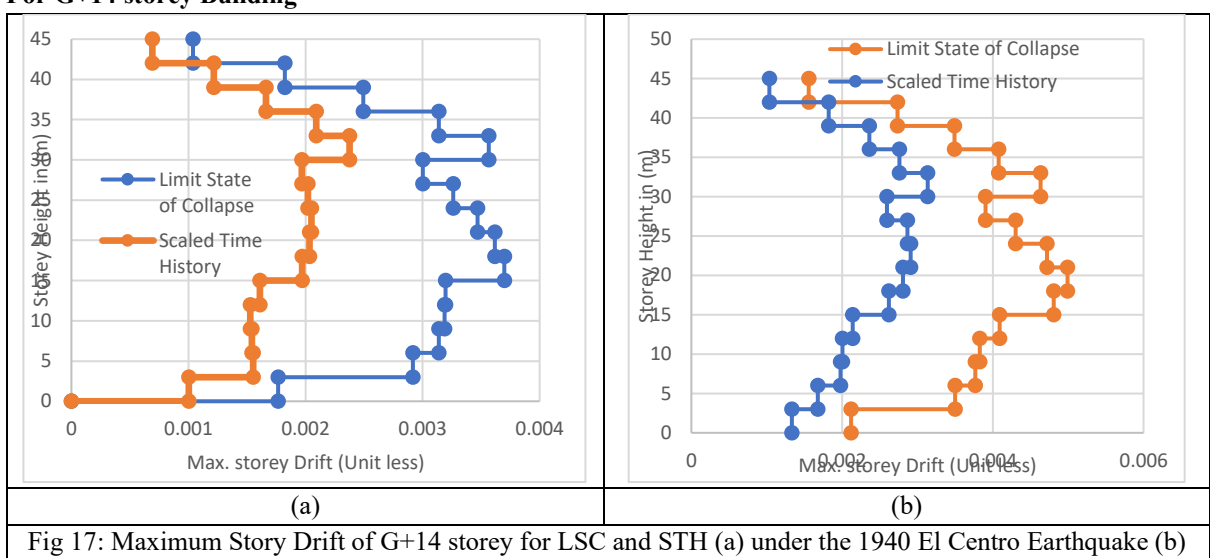


Fig 17: Maximum Story Drift of G+14 storey for LSC and STH (a) under the 1940 El Centro Earthquake (b) under the 1994 Northridge Earthquake

The graph shows the maximum story drift values across different story heights of the building under the 1940 El Centro & 1994 Northridge Earthquake. The drift starts low at the base and gradually increases, reaching a peak at 6th floor and 0.0237 at 11th story for LSC and STH respectively. After this point, the drift slightly decreases towards the top. These values help identify the areas where the building experiences the most lateral movement, crucial for evaluating its stability under lateral forces like wind or seismic activity. The structure undergoes greater lateral deformation under Northridge, particularly in the critical lower-mid stories.

For G+24 storey Building

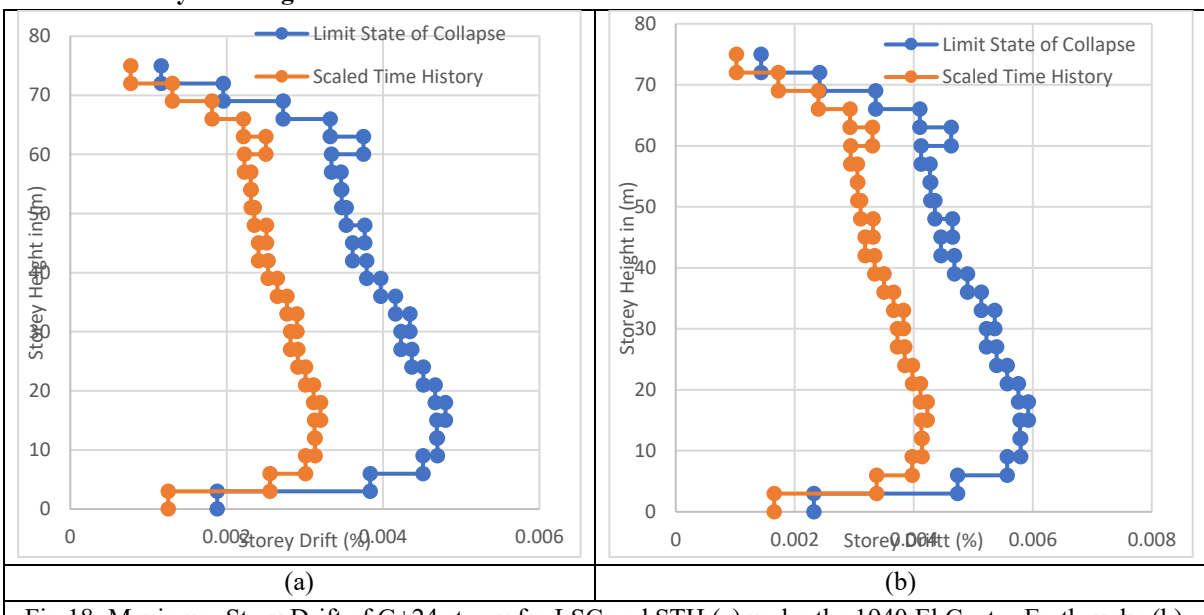


Fig 18: Maximum Story Drift of G+24 storey for LSC and STH (a) under the 1940 El Centro Earthquake (b) under the 1994 Northridge Earthquake

The graph shows the maximum story drift values across different story heights of the building. The drift starts low at the base and gradually increases, reaching a peak at 6th floor story for both LSC and STH case. After this point, the drift slightly decreases towards the top. These values help identify the areas where the building experiences the most lateral movement, crucial for evaluating its stability under lateral forces like wind or seismic

activity. The structure undergoes greater lateral deformation under Northridge, particularly in the critical lower portion of the building.

For G+24 storey Building

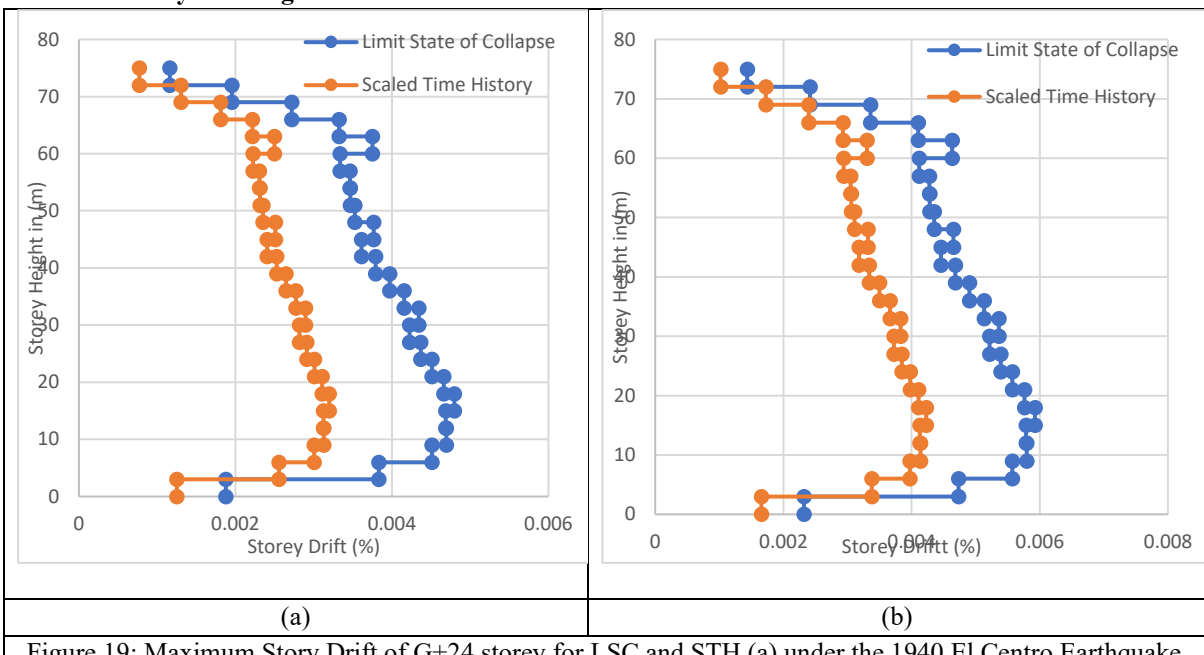


Figure 19: Maximum Story Drift of G+24 storey for LSC and STH (a) under the 1940 El Centro Earthquake (b) under the 1994 Northridge Earthquake

The figure 17, 18 and 19 shows the maximum story drift values across different story heights of the building. The drift starts low at the base and gradually increases, reaching a peak of approximately 0.004769 at 2nd floor and 0.002829 at 2nd floor for LSC and STH respectively for G+4 storey building, 0.0037 at 6th floor and 0.0237 at 11th story for LSC and STH respectively for G+14 storey building and 0.0037 at 6th floor and 0.0237 at 11th story for LSC and STH respectively for G+24 storey building. After this point, the drift slightly decreases towards the top. These values help identify the areas where the building experiences the most lateral movement, crucial for evaluating its stability under lateral forces like wind or seismic activity.

Story Shears details using Etabs software

For G+4 storey Building

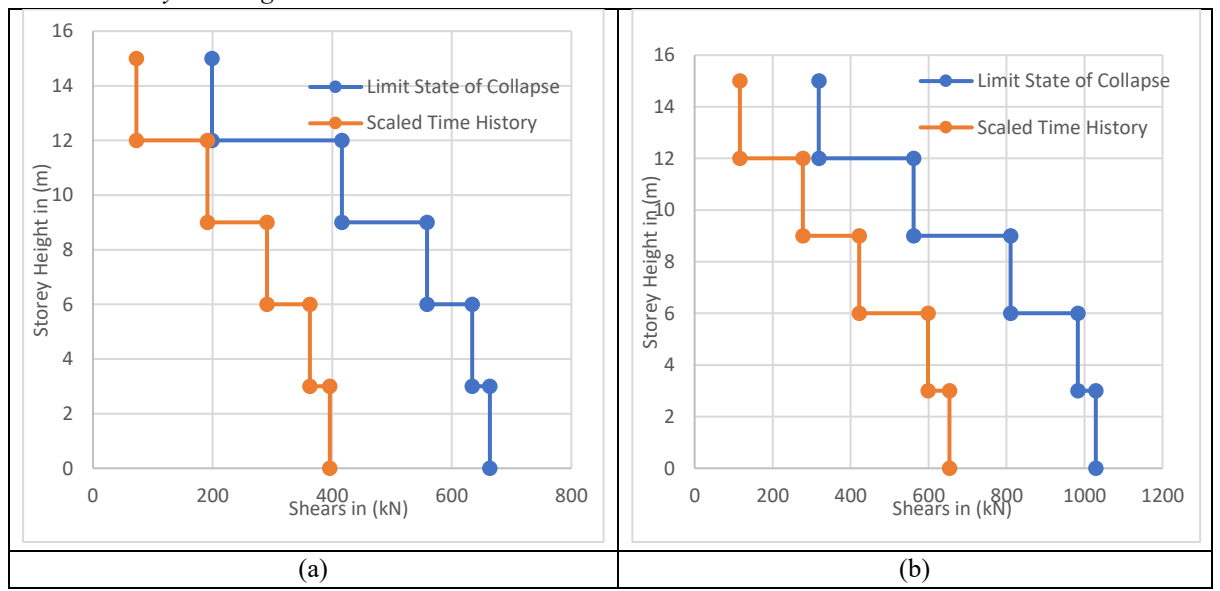


Figure 20: Maximum Story Drift of G+4 storey for LSC and STH (a) under the 1940 El Centro Earthquake (b) under the 1994 Northridge Earthquake

For the fifteen-story building, the Elcentro earthquake produces shear forces ranging from 196.48 kN at the terrace to 655.54 kN at the base in the LSC case, and 72.01 kN to 393.08 kN in the STH case. The Northridge earthquake yields slightly higher values 198.96 kN to 679.56 kN in LSC and 82.65 kN to 393.52 kN in STH. Although the increases are modest, Northridge imposes consistently greater lateral shear across the height. These results highlight the need for robust detailing and redundancy in lateral load-resisting systems to ensure reliable seismic performance.

For G+14 storey Building

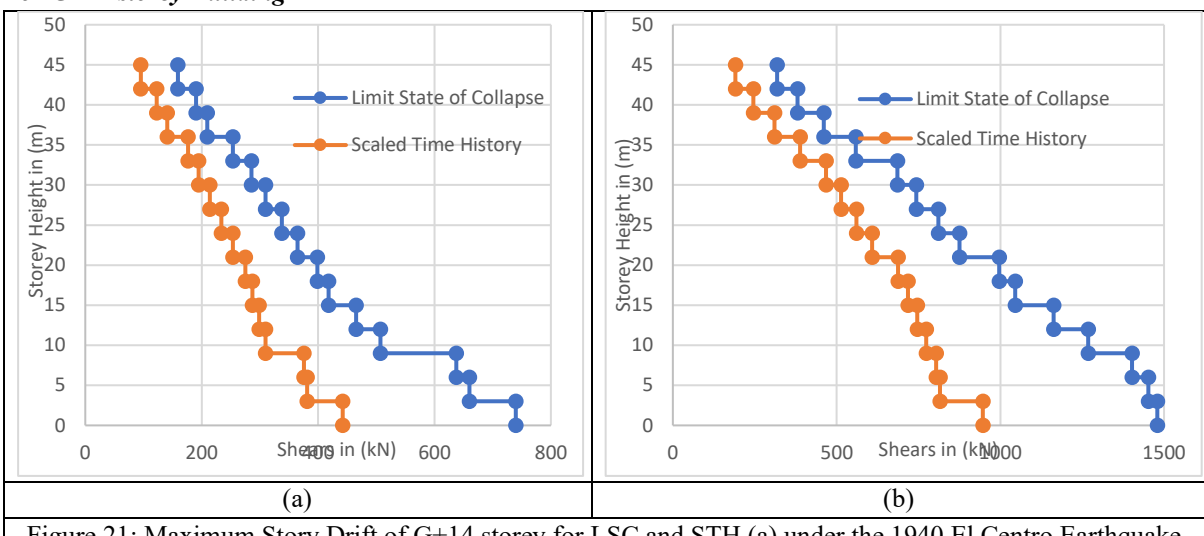


Figure 21: Maximum Story Drift of G+14 storey for LSC and STH (a) under the 1940 El Centro Earthquake (b) under the 1994 Northridge Earthquake

For the fifteen-story building, Elcentro produces shear forces of 159.21 kN at the terrace to 739.72 kN at the base (LSC) and 95.47 kN to 442.32 kN (STH), while Northridge yields 318.41 kN to 1479.45 kN (LSC) and 190.94 kN to 946.56 kN (STH), nearly double Elcentro's values. The increase is uniform from top to base, showing higher cumulative lateral forces under Northridge. Maximum displacements reach 104.98 mm for Elcentro and 149.29 mm for Northridge at the top story. ABAQUS results closely match ETABS time history analysis, confirming consistency without load combinations.

For G+24 storey Building

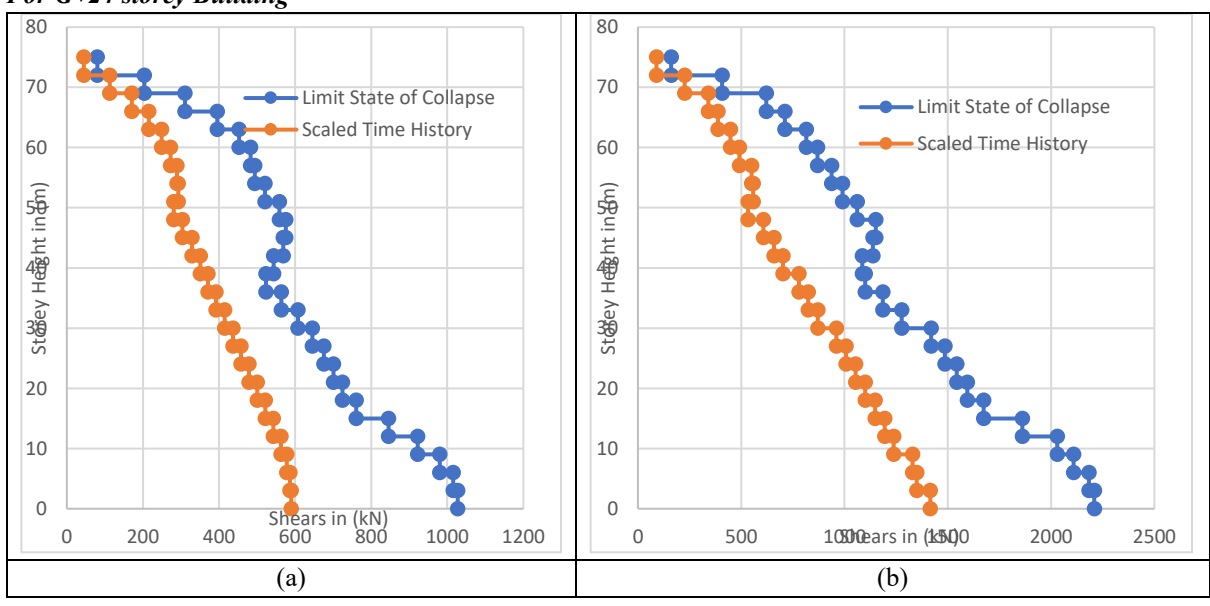


Figure 22: Maximum Story Drift of G+24 storey for LSC and STH (a) under the 1940 El Centro Earthquake (b) under the 1994 Northridge Earthquake

For the fifteen-story building, Elcentro produces shear forces of 80.32 kN to 1027.40 kN (LSC) and 44.82 kN to 589.76 kN (STH), while Northridge induces 160.63 kN to 2208.90 kN (LSC) and 89.64 kN to 1415.41 kN (STH), more than double Elcentro's values. Shear increases consistently from top to base, highlighting higher cumulative lateral loads under Northridge. For G+4, G+14, and G+24 buildings, terrace-to-base shears range from 72.56–666.77 kN, 64.97–854.27 kN, and 72.56–666.77 kN, respectively, showing cumulative lateral effects. Base shear time history under Elcentro peaks at 503.967 kN at 4.77 s with 0.349g acceleration at 2.175 s, followed by damped oscillations, reflecting seismic energy dissipation.

Landfill Site (LFS) with and Without Pile using ABAQUS

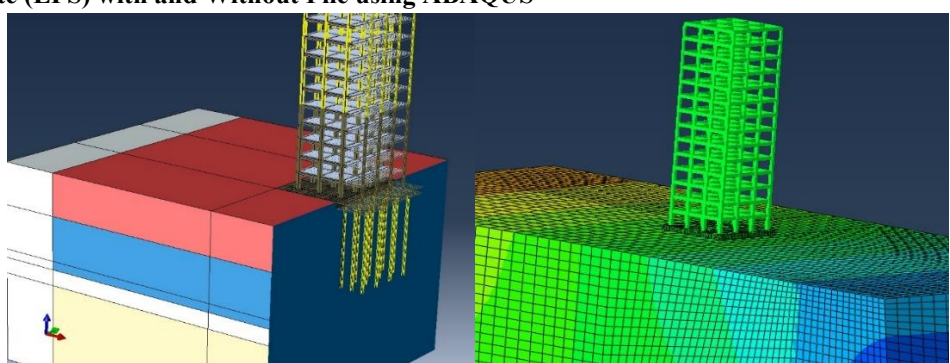


Figure 38: RCC Structure on Multilayer soil analysed with and without piles

Maximum Story Displacement

The graph following graph of G+4 storey, G+14 storey & G+24 storey buildings illustrates the maximum story displacement of a multistory building considering two scenarios: one with piles and one without piles. The data demonstrates that the inclusion of piles significantly reduces the displacement across all stories of the building.

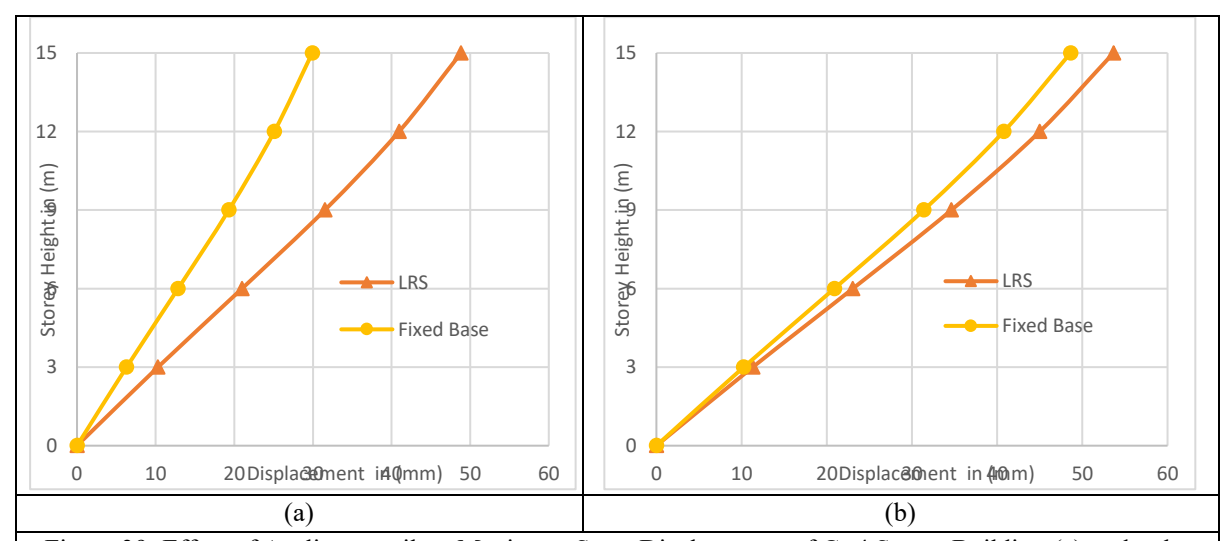
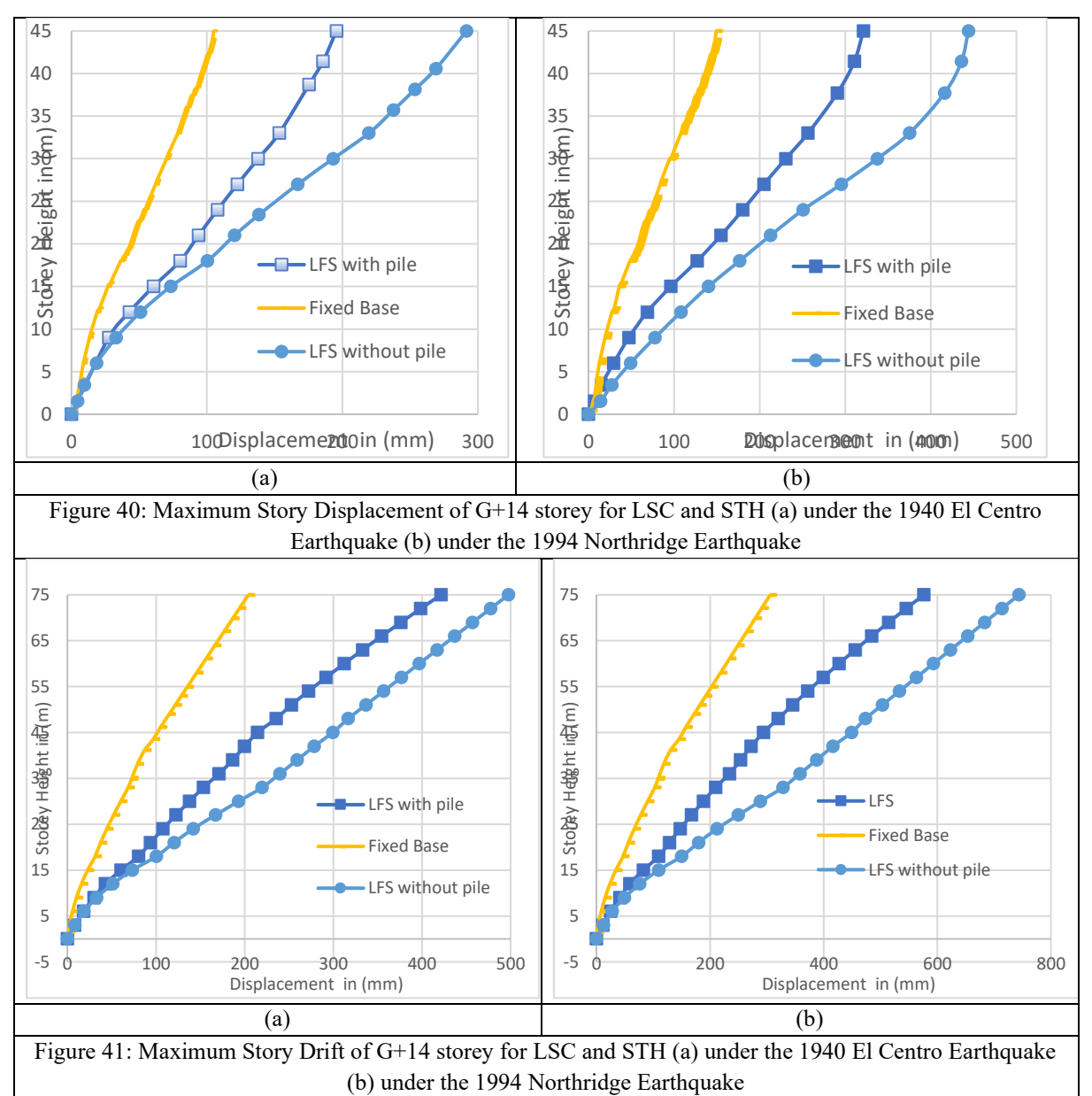


Figure 39: Effect of Acclimate soil on Maximum Story Displacement of G+4 Storey Building (a) under the 1940 El Centro Earthquake (b) under the 1994 Northridge Earthquake



Buildings on Landfill Sites (LFS) show significantly higher lateral displacements due to soft soil conditions, with G+4, G+14, and G+24 storeys experiencing up to 68.95 mm, 388.05 mm, and 576.22 mm under El Centro and Northridge earthquakes without piles. Introducing piles reduces displacements but amplification remains notable, e.g., 166.23–655.88 mm across building heights. This highlights the critical impact of soft soils on seismic performance, emphasizing the need for soil-structure interaction analysis and careful foundation design.

ISSN: 1001-4055 Vol. 46 No. 04 (2025)

Maximum Story Drift considering SSI Effect for Landfill Site (LFS)

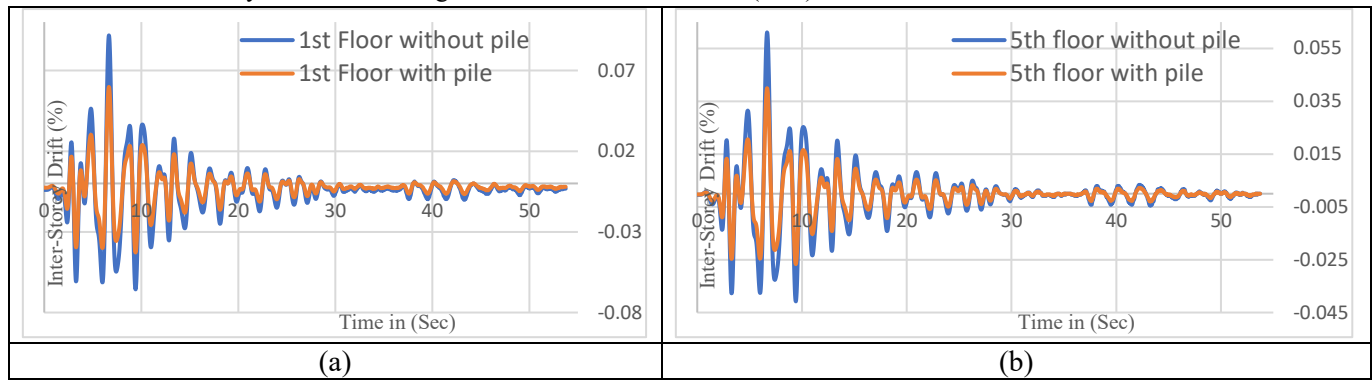


Figure 42: Maximum Story Drift Comparison with and without Piles (a) 1st floor, (b) 5th floor under the 1940 Elcentro Earthquake.

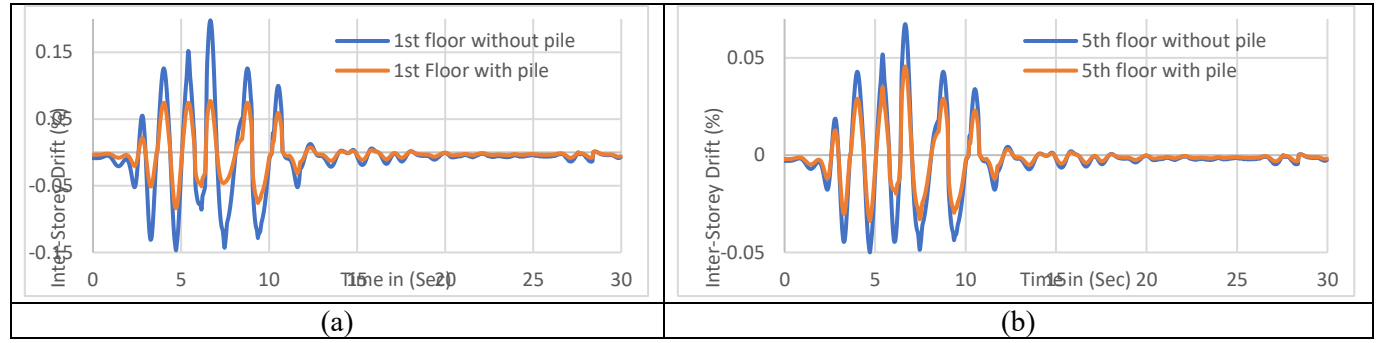


Figure 43: Maximum Story Drift Comparison with and without Piles (a) 1st floor, (b) 5th floor under the 1994 Northridge Earthquake.

Mid Rise Building (G+14 Storey Building)

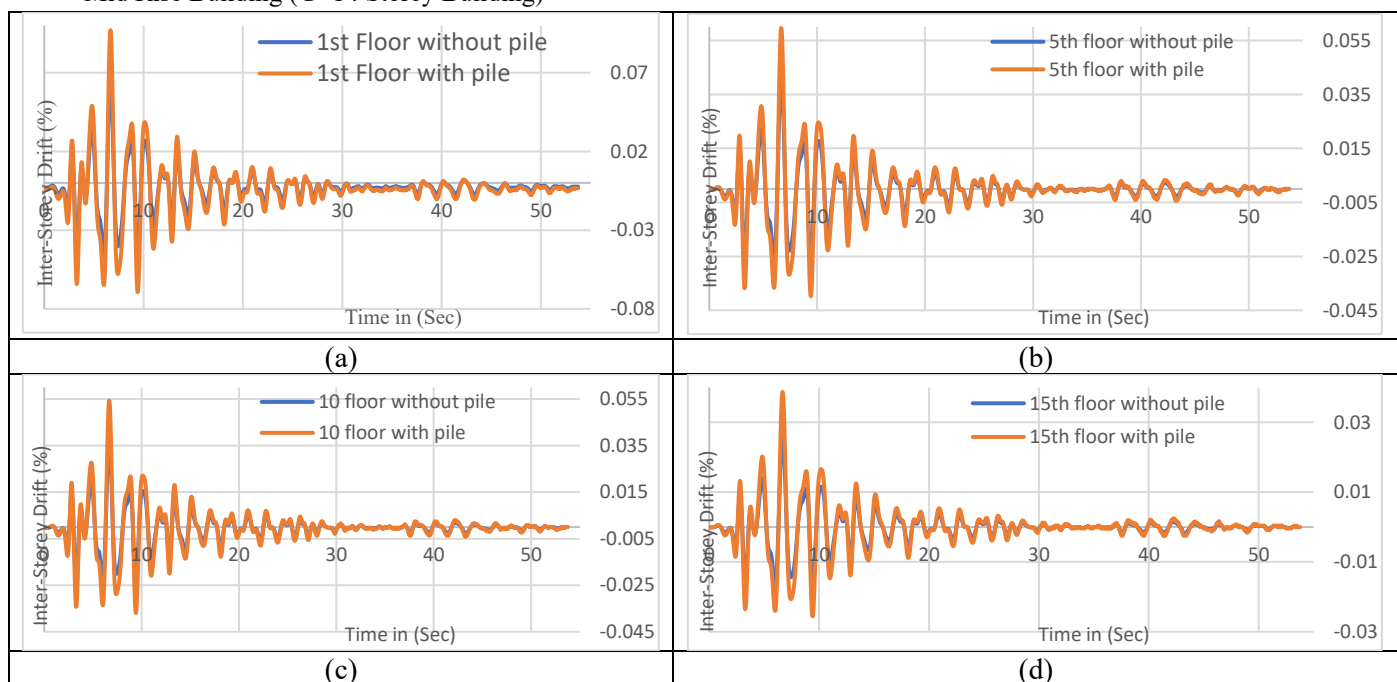


Figure 44: Maximum Story Drift Comparison with and without Piles: (a) 1st floor, (b) 5th floor, (c) 10th floor, (d) 15th floor under the 1940 Elcentro Earthquake.

ISSN: 1001-4055

Vol. 46 No. 04 (2025)

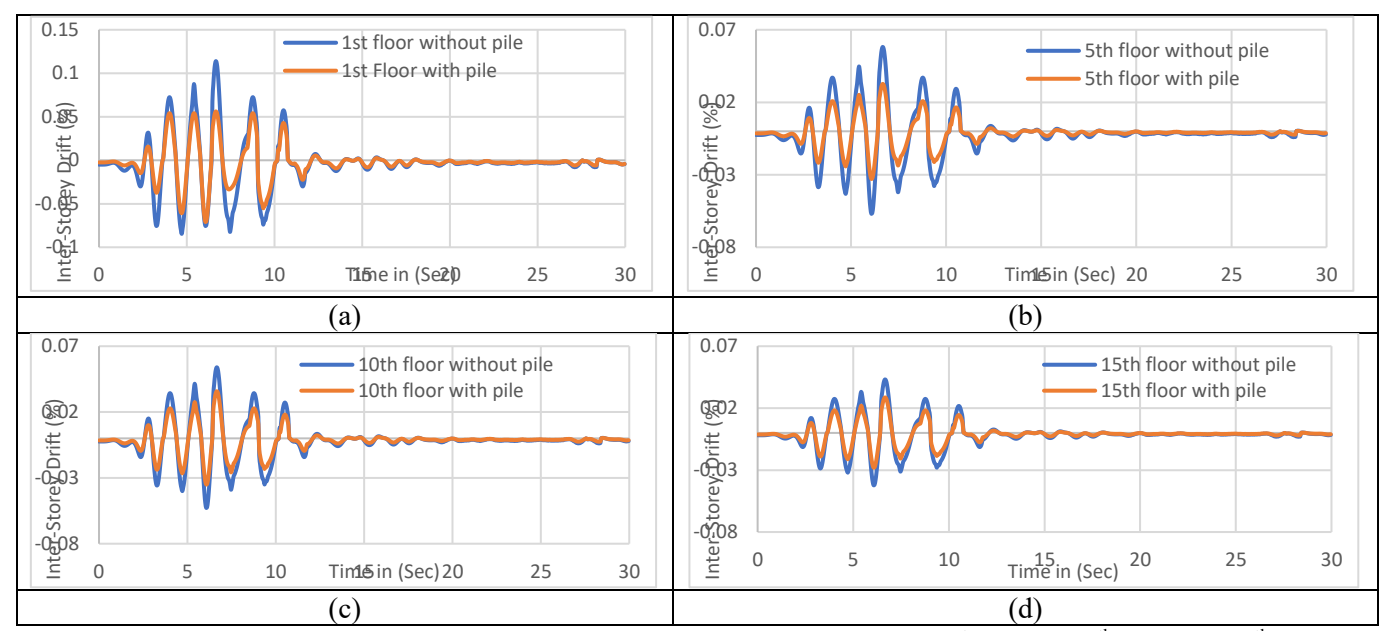


Figure 45: Maximum Story Drift Comparison with and without Piles: (a) 1st floor, (b) 5th floor, (c) 10th floor, (d) 15th floor under the 1994 Northridge Earthquake.

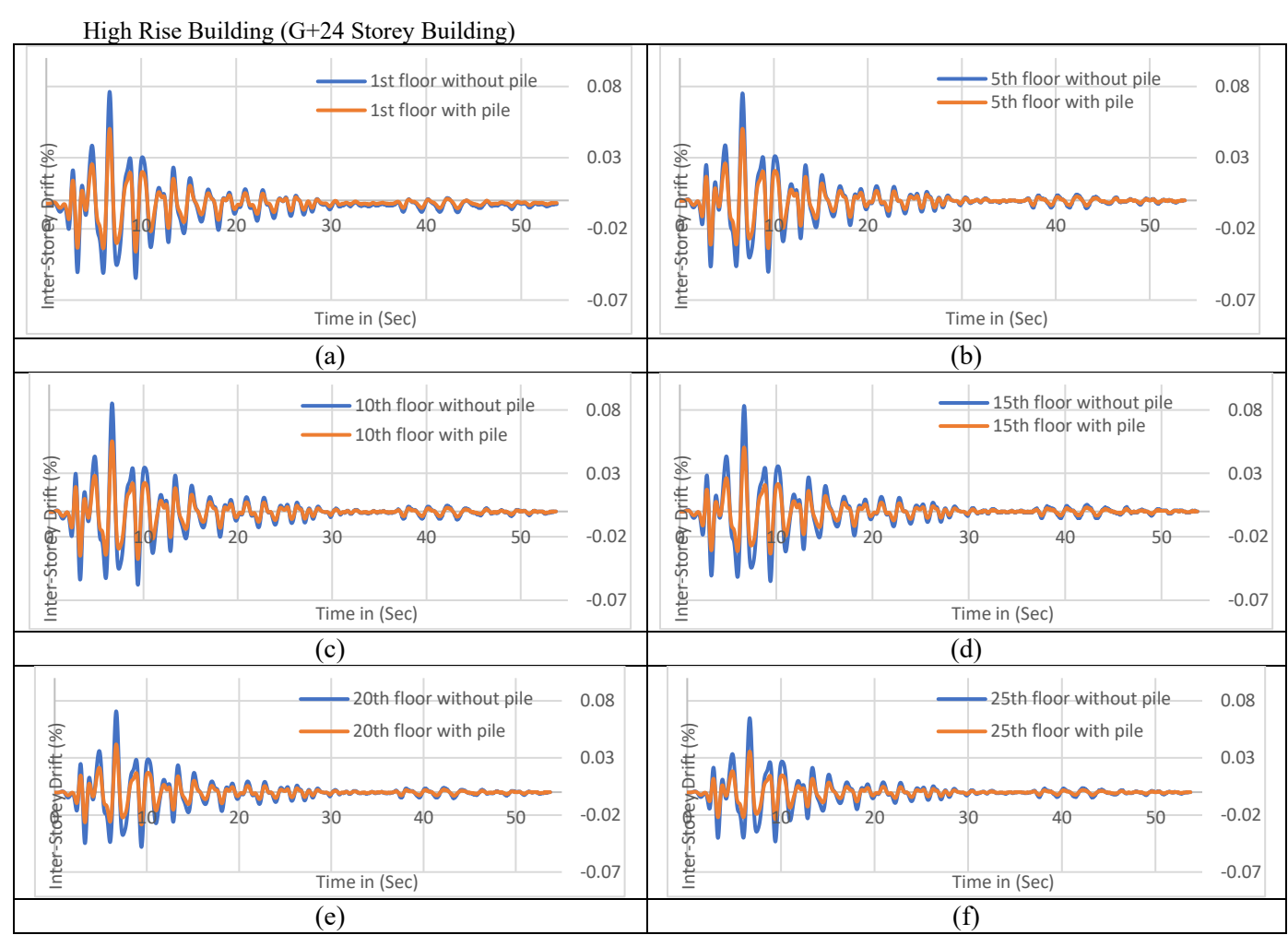


Figure 46: Maximum Story Drift Comparison with and without Piles: (a) 1st floor, (b) 5th floor, (c) 10th floor, (d) 15th floor, (e) 20th floor, (f) 25th floor under the 1940 Elcentro Earthquake.

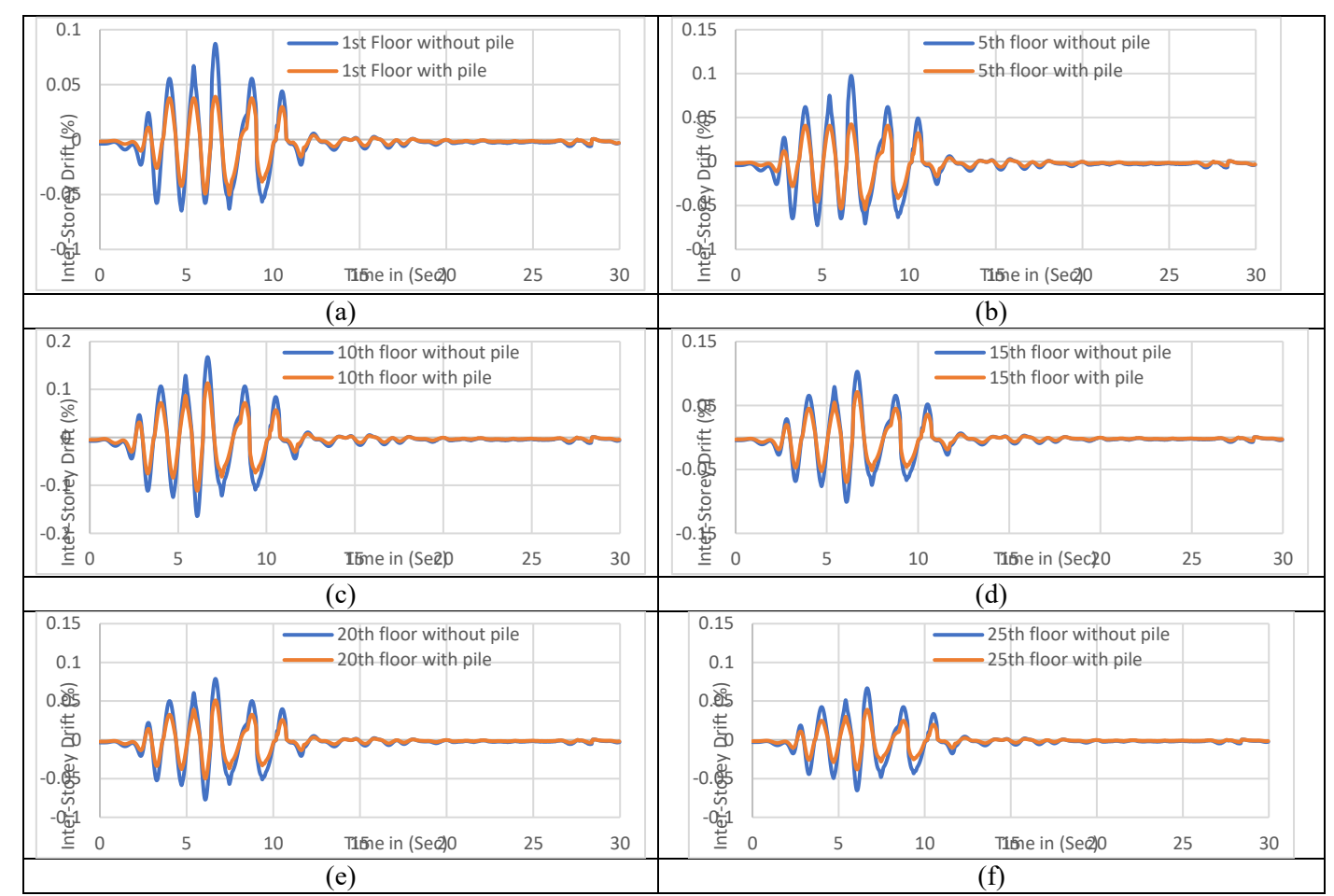


Figure 47: Maximum Story Drift Comparison with and without Piles: (a) 1st floor, (b) 5th floor, (c) 10th floor, (d) 15th floor, (e) 20th floor, (f) 25th floor under the 1994 Northridge Earthquake.

On Landfill Sites (LFS), interstorey drift is highest at the base for G+4 buildings and around mid-height (10th floor) for G+14 and G+24 buildings, with Northridge causing greater drift than El Centro. Pile foundations reduce drift significantly at lower floors but less so at upper levels. Despite piles, drift on LFS often exceeds the IS 1893 limit of 0.004, especially in low-density soils.

Story acceleration considering SSI analysis for Landfill Site (LFS)

Low Rise Building (G+4 Storey Building)

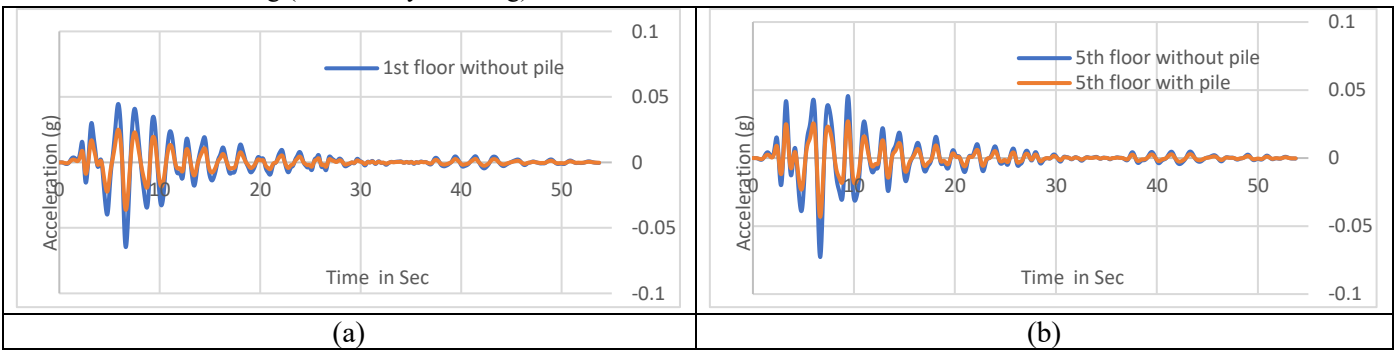


Figure 48: Maximum Story Acceleration Comparison with and without Piles: (a) Base, (b) 1st floor, (b) 5th floor under the 1940 Elcentro Earthquake.

ISSN: 1001-4055 Vol. 46 No. 04 (2025)

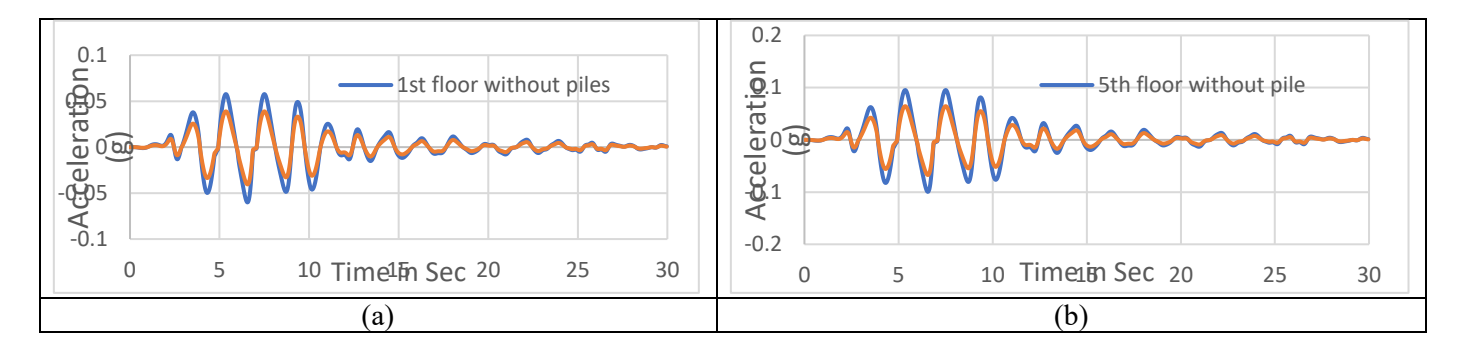


Figure 49: Maximum Story Acceleration Comparison with and without Piles: (a) Base, (b) 1st floor, (b) 5th floor under the 1994 Northridge Earthquake.

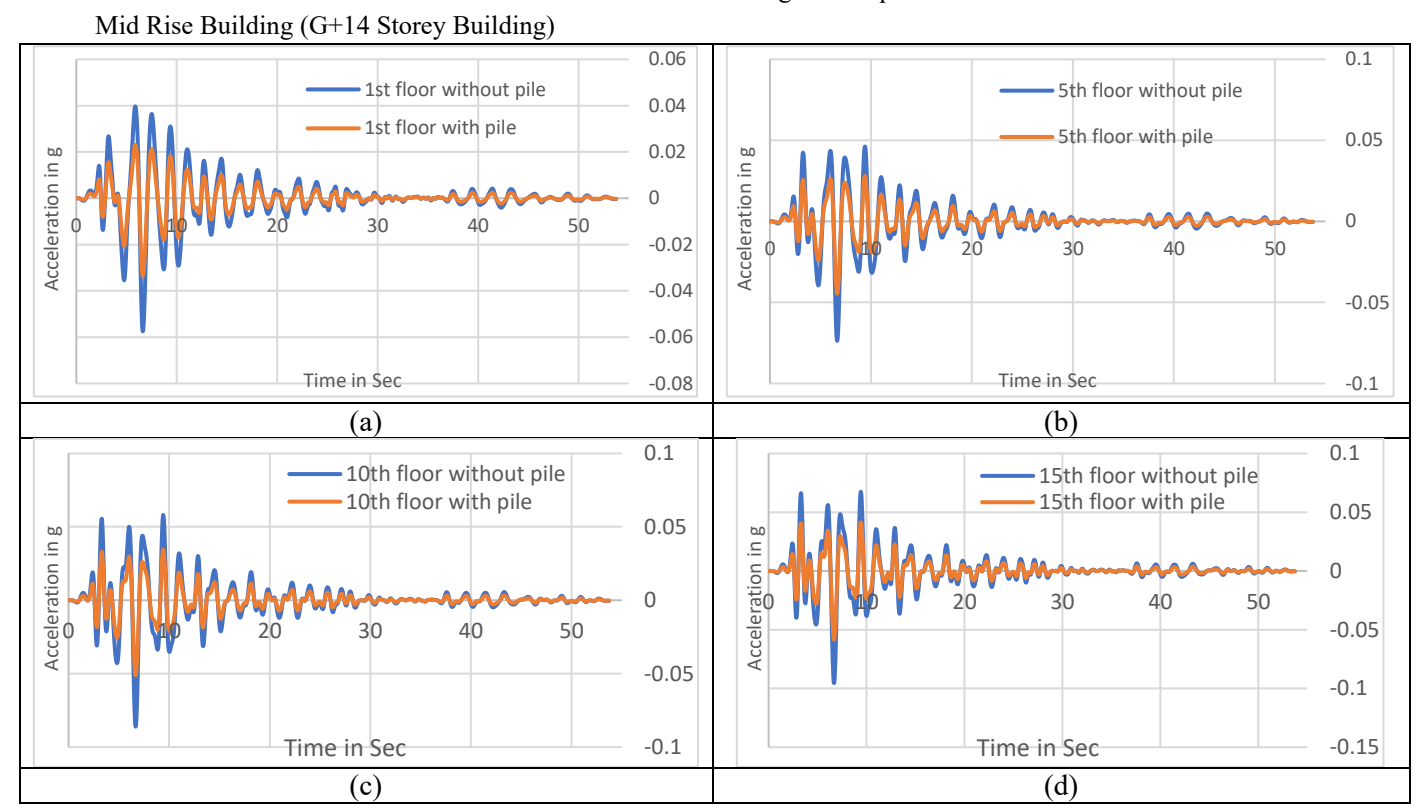
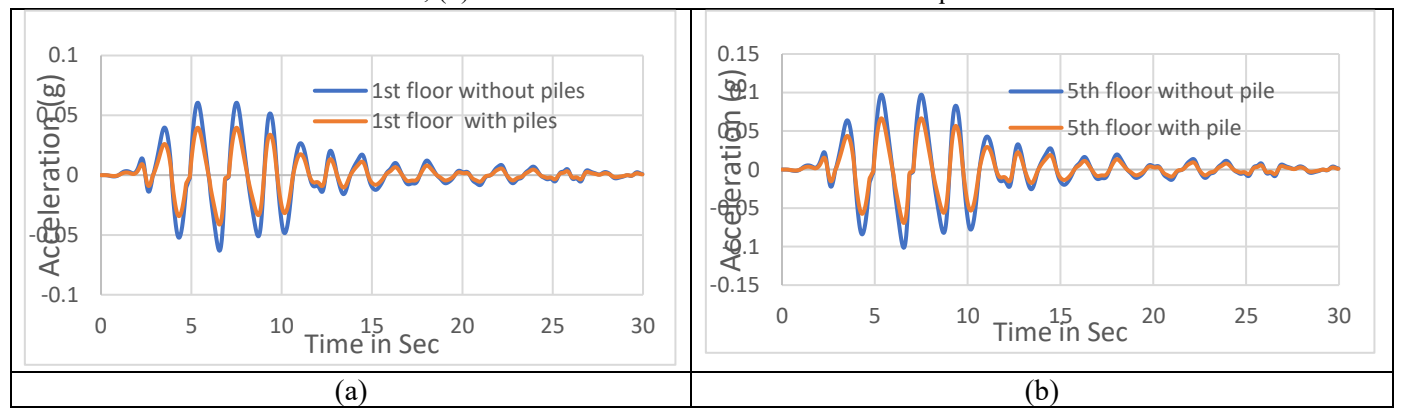


Figure 50: Maximum Story Acceleration Comparison with and without Piles: (a) Base, (b) 5th floor, (c) 10th floor, (d) 15th floor under the 1940 Elcentro Earthquake.



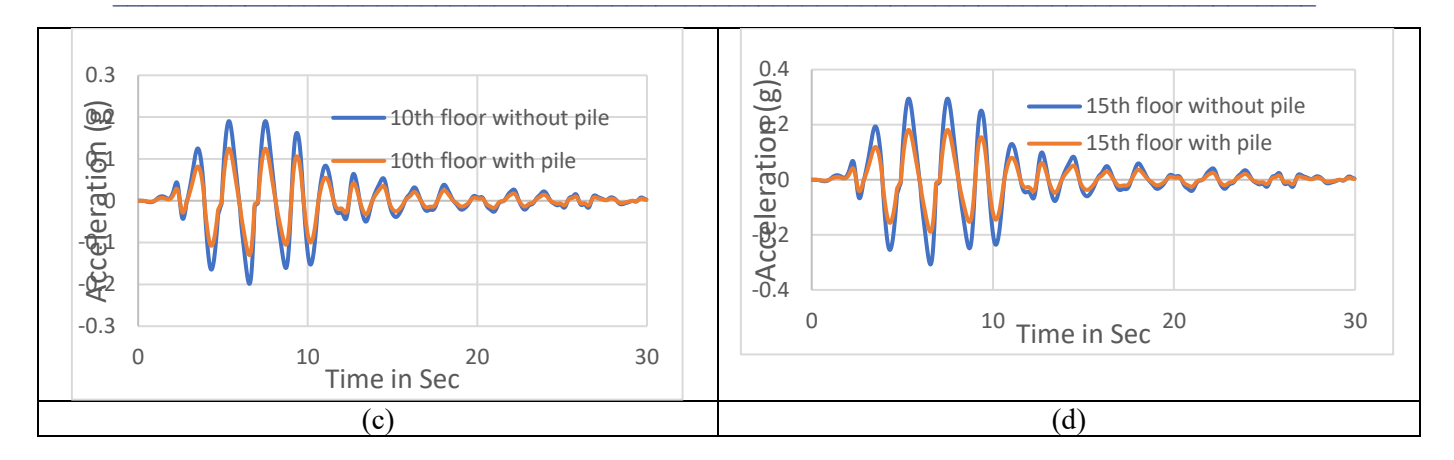


Figure 51: Maximum Story Acceleration Comparison with and without Piles: (a) Base, (b) 5th floor, (c) 10th floor, (d) 15th floor under the 1994 Northridge Earthquake.

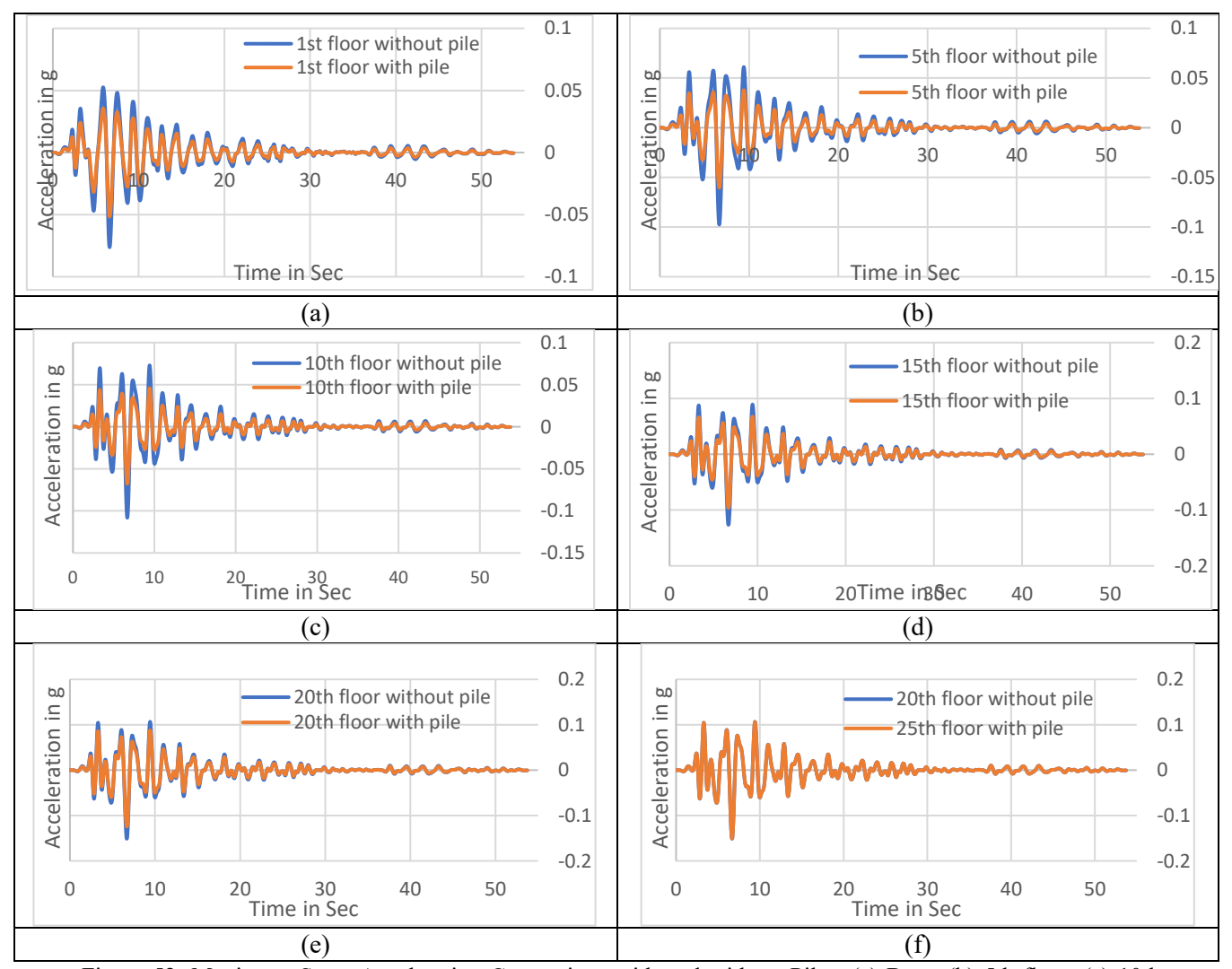


Figure 52: Maximum Story Acceleration Comparison with and without Piles: (a) Base, (b) 5th floor, (c) 10th floor, (d) 15th floor, (e) 20th floor, (f) 25th floor under the 1940 Elcentro Earthquake.

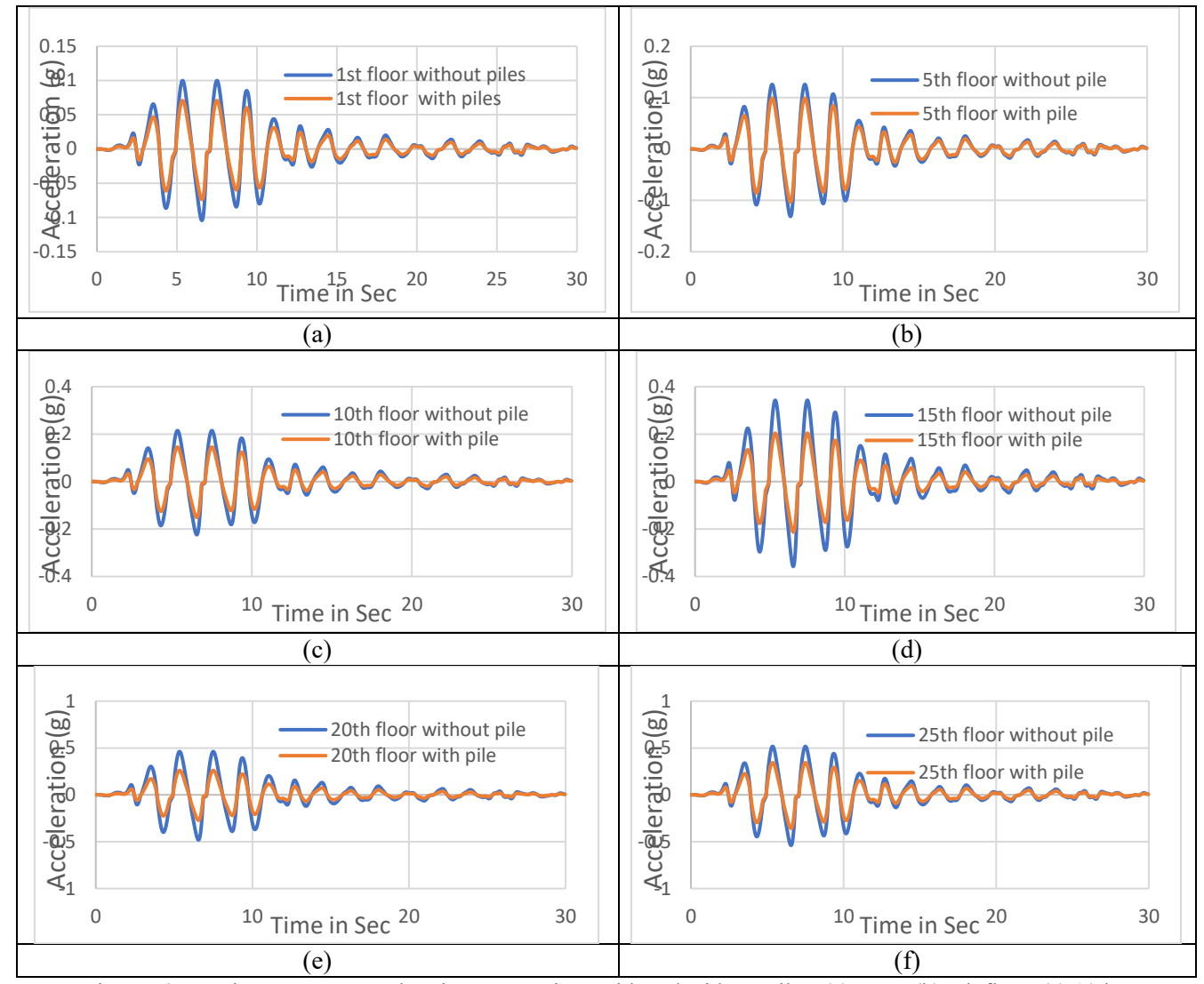


Figure 53: Maximum Story Acceleration Comparison with and without Piles: (a) Base, (b) 5th floor, (c) 10th floor, (d) 15th floor, (e) 20th floor, (f) 25th floor under the 1994 Northridge Earthquake.

Figures 51–53 compare maximum story acceleration for G+4, G+14, and G+24 buildings with and without piles at selected floors under seismic loading. Piles significantly reduce peak acceleration at the base and lower floors, effectively dampening seismic energy. At higher floors, the difference decreases, showing reduced pile influence with height. Overall, piles lower the building's seismic response, enhancing safety and reducing potential structural damage.

Conclusions Drawn from the Study

The maximum story displacement from ABAQUS closely matches the ETABS time history analysis, confirming the reliability of both tools for dynamic seismic analysis when using time history methods. The introduction of pile foundations reduced the maximum story displacement for mid rise (G+14 storey) Building and high rise (G+24 storey) Building demonstrating a significant improvement in the building's seismic performance. The substantial difference in displacement values with and without piles underscores the importance of scenario-specific analysis to accurately predict structural performance under seismic conditions. The acceleration increases with building height, reaching its peak at the top story. The maximum ground acceleration of the El Centro Earthquake was 0.281 g, while the top story experienced 0.0882 g, about 31.38% of the earthquake's PGA for G+4 storey Building, for G+14 storey Building- top story experienced 0.174 g, about 61.9% of the earthquake's PGA and for G+24 storey Building experienced 0.4116 g, about 141.47% of the earthquake's PGA.

Tuijin Jishu/Journal of Propulsion Technology

ISSN: 1001-4055 Vol. 46 No. 04 (2025)

Declarations:

Funding

The authors declare that no funds, grants, or other support were received during the preparation of this manuscript.

Data availability Statement

The data used for preparing the charts, graphs, and other analyses in this manuscript are available upon request. We are happy to share all relevant datasets and supporting materials to ensure transparency and reproducibility of the findings presented in the manuscript.

Competing Interests

The authors have no relevant financial or non-financial interests to disclose

Author Contributions

Mr. Pruthviraj S. R: Conceptualized the study, conducted the research, and performed the soil-structure interaction (SSI) analysis. Utilized advanced tools such as ETABS, CSI Detailing, and ABAQUS CAE for the design and analysis of seismic behavior of multistorey buildings constructed on MSW landfill site. Led the preparation and writing of the manuscript, integrating results from simulations and validating the findings with experimental data and comparisons with previous studies. Mr. Pruthviraj S. R. was the principal contributor to the work.

Dr. K. Manjunatha: Provided guidance on the seismic analysis methods and interpretation of results. Assisted in refining the research approach and contributed to the validation of findings by comparing them with prior studies. Dr. K. Manjunatha also offered critical feedback during manuscript preparation, ensuring the study's methodology and conclusions were sound.

Dr. C. M. Ravi Kumar: Guided the research on soil properties, particularly in relation to the Changi East land reclamation project, and advised on how reclaimed soil impacts the seismic response of buildings. Dr. C. M. Ravi Kumar also provided valuable insights and suggestions during the manuscript review, contributing to the final interpretation of results and ensuring the study's relevance to the field of Civil Engineering.

REFERENCES

- 1. Abdul Ahad Faizan, O.K. (2019). Seismic Non-Linear Time History Analysis of Multi Storied RCC Residential Building Subjected to Different Earthquake Ground Motions Using ETABS. International Journal of Advances in Mechanical and Civil Engineering, 6(4).
- 2. Algamati, M. et al. (2023). Studying and Analyzing the Seismic Performance of Concrete Moment-Resisting Frame Buildings. Civileng, 4(1), 34–54. https://doi.org/10.3390/civileng4010003
- 3. Bapir, B. et al. (2023). Soil-Structure Interaction: A State-of-the-Art Review of Modeling Techniques and Studies on Seismic Response of Building Structures. Frontiers in Built Environment, 9. https://doi.org/10.3389/fbuil.2023.1120351
- 4. Bariker, P. & Kolathayar, S. (2022). *Dynamic Soil Structure Interaction of a High-Rise Building Resting over a Finned Pile Mat. Infrastructures*, 7(10). https://doi.org/10.3390/infrastructures7100142
- 5. Bowles, J.E. (1996). Foundation Analysis and Design. McGraw-Hill Companies, Inc.
- 6. Choudhury, D., Phanikanth, V. S., Mhaske, S. Y., Phule, R. R., & Chatterjee, K. (2015). Seismic Liquefaction Hazard and Site Response for Design of Piles in Mumbai City. Indian Geotechnical Journal, 45(1), 62–78. https://doi.org/10.1007/s40098-014-0108-4
- 7. Dixit, J., Dewaikar, D. M., & Jangid, R. S. (2012). *Soil Liquefaction Studies at Mumbai City. Natural Hazards*, 63(2), 375–390. https://doi.org/10.1007/s11069-012-0154-0
- 8. Eurocode 8 (2011). Design of Structures for Earthquake Resistance Part 1. European Union.
- 9. FEMA P-2091 (2020). A Practical Guide to Soil-Structure Interaction. Applied Technology Council. www.ATCouncil.org
- 10. Gazetas, G., & Mylonakis, G. (1998). Seismic Soil-Structure Interaction: New Evidence and Emerging Issues. Geotechnical Earthquake Engineering and Soil Dynamics, pp. 1–56.
- 11. Hasan, A. et al. (2023). Nonlinear Time History Analysis for Seismic Effects on Reinforced Concrete Building. Nigerian Journal of Technological Development, 19(4), 391–399. https://doi.org/10.4314/njtd.v19i4.12

Tuijin Jishu/Journal of Propulsion Technology

ISSN: 1001-4055 Vol. 46 No. 04 (2025)

- 12. IS 1893 Part-1 (2016). Criteria for Earthquake Resistant Design of Structures. Bureau of Indian Standards, New Delhi.
- 13. IS 2911 (Part-1/Sec-2) (2010). *Design and Construction of Pile Foundations*. Bureau of Indian Standards, New Delhi.
- 14. IS 456 (2000). Plain and Reinforced Concrete Code of Practice. Bureau of Indian Standards, New Delhi.
- IS 875 Part-1 (1987). Code of Practice for Design Loads (Dead Loads). Bureau of Indian Standards, New Delhi.
- 16. IS 875 Part-2 (1987). Code of Practice for Design Loads (Other than Earthquake). Bureau of Indian Standards, New Delhi.
- 17. Kramer, S.L. (1996). Geotechnical Earthquake Engineering. Prentice-Hall.
- 18. Matinmanesh, H. & Asheghabadi, M.S. (2011). Seismic Analysis on Soil-Structure Interaction of Buildings Over Sandy Soil. Procedia Engineering, 14, 1737–1743. https://doi.org/10.1016/j.proeng.2011.07.218
- 19. Mhaske, S. Y. & Choudhury, D. (2011). *Geospatial Contour Mapping of Shear Wave Velocity for Mumbai City. Natural Hazards*, 59(1), 317–327. https://doi.org/10.1007/s11069-011-9758-z
- 20. Mylonakis, G. & Gazetas, G. (2000). Seismic Soil-Structure Interaction: Beneficial or Detrimental?. Journal of Earthquake Engineering, 4(3), 277–301. https://doi.org/10.1080/13632460009350372
- 21. Patil, A.S. & Kumbhar, P.D. (2013). Time History Analysis of Multistoried RCC Buildings for Different Seismic Intensities. International Journal of Structural and Civil Engineering Research, 2(3), 195–201.
- 22. Pitchumani, K. & Islam, A. (2021). Reclamation and Ground Improvement of Soft Marine Clay for Development of Offshore Terminal 4, JNPT, Navi Mumbai. Indian Geotechnical Journal, 51, 502–519. https://doi.org/10.1007/s40098-021-00521-y
- 23. Pujol, G. & Roca, A. (1992). Soil-Structure Interaction and Seismic Performance in Mexico City. Earthquake Engineering Research Institute (EERI).
- 24. Ramdev, P. & Barbude, P.R. (2021). Dynamic Analysis of Multistory Structure using Linear Time History Analysis. International Journal of Engineering Research in Mechanical and Civil Engineering (IJERMCE), 6(11), 6–10.
- 25. Rayhani, M.H.T. & El Naggar, H. (2008). *Physical and Numerical Modeling of Dynamic Soil-Structure Interaction*, pp. 1–11. https://doi.org/10.1061/40975(318)127
- 26. Sam Helwani (2014). *Applied Soil Mechanics with Abaqus Applications*. John Wiley & Sons. https://doi.org/10.1007/978-3-642-41714-6 12322
- 27. Shekhar, S., Tripathi, S.M., & Ram, S. (2022). Effect of Soil Structure Interaction on Seismic Response of Buildings. Lecture Notes in Civil Engineering, 154(8), 39–48. https://doi.org/10.1007/978-981-16-1993-9 5
- 28. Tabatabaiefar, S., Fatahi, B. & Samali, B. (2014). Numerical and Experimental Investigations on Seismic Response of Building Frames Under Influence of Soil-Structure Interaction. Advances in Structural Engineering, 17(1), 109–130. https://doi.org/10.1260/1369-4332.17.1.109
- 29. Van Nguyen, Q., Fatahi, B., & Hokmabadi, A.S. (2017). *Influence of Size and Load-Bearing Mechanism of Piles on Seismic Performance of Buildings Considering Soil—Pile—Structure Interaction. International Journal of Geomechanics*, 17(7). https://doi.org/10.1061/(asce)gm.1943-5622.0000869
- 30. Visuvasam, J. & Chandrasekaran, S.S. (2019). Effect of Soil–Pile–Structure Interaction on Seismic Behaviour of RC Building Frames. Innovative Infrastructure Solutions, 4(1), 0–19. https://doi.org/10.1007/s41062-019-0233-0
- 31. Wolf, J.P. (1985). Dynamic Soil-Structure Interaction. Prentice-Hall.